TRACKING THE "POORNESS" OF A LINEAR SHAPED CHARGE

F. Rondot

French German Research Institute (ISL), BP 70034, 68301 Saint-Louis, France

A combined experimental and numerical study was carried out to understand why some linear shaped charges had failed qualifying tests for space applications.
Instrumented tests were performed on two different batches. Flash X-Rays revealed that the suspicious specimens form veils with an anomaly of curvature. Finally, two parallels drills are successively generated into a witness target.
By means of Euler numerical simulations with a grid density of 400 cells per square millimeter, the results of a calibrated defect were examined. The computations have shown that a $1/10^{th}$-mm misalignment of the explosive charge with the liner was enough to perturb in a significant way the shaping of the veil. With regard to the stand-off, several drills were then created into a thick target. We carefully do not claim to have identified the imperfection responsible for the anomalies observed during experiments.
In a last step, perforation capacities of this defective linear shaped charge were compared to the reference case. It came out that the effects are less obvious with a thin witness target made of high hardness steel at a functional stand-off of 6 mm. Even if the process of interaction differs, the defective charge keeps a perforation capacity similar to the reference.

INTRODUCTION

Europe's heavy-lift launcher Ariane 5 is fitted with linear shaped charge (LSC) to neutralize its solid booster stages. In a near past, some devices have failed the qualifying tests. Two shallow cutting lines were observed into a witness aluminum plate.

The study combined instrumented experiments and fine numerical simulations to try to understand and explain the anomalies. Taking into account a realistic configuration, the perforation capacities are then discussed.

INSTRUMENTED TESTS

Two different batches were tested. The experimental set-up is shown on Figure 1. The diagnostics were based upon X-Ray pictures taken from a generator of 750 kV that delivers flashes with duration of about 20 nanoseconds. The LSC has a section of 17x17 mm². The linear explosive loading is 46 g/m for a linear mass of lead of 1286 g/m. To discern the anomalies of the veils, front X-Ray pictures had to be delayed and the aluminum witness block had to be removed up to a stand-off of 350 mm.

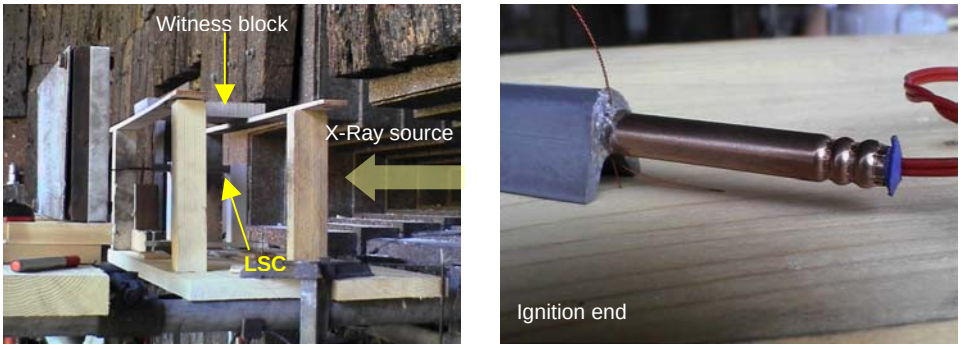

Figure 1. Overview of the experimental set-up (left) and instantaneous electrical detonator (right)

Figure 2 reveals a sharp curvature of the veil from the suspicious batch #2. It seems that the double drill obtained on the target is not the consequence of a forked veil but rather these of a non straight veil: the front part makes a first drill and the middle part which is misaligned creates a second parallel drill.

Figure 2. Front X-Rays show a suitable veil from batch #1 (above) and a poor veil from batch #2 (bottom)

Figure 3 exhibits the cutting line(s) into the witness block of aluminum alloy. The specimens of batch #1 generate a single drill. A double drill was observed with each specimen of the defective device. The distance between the two drills increased with the stand-off (*SO*), from 7 mm at *SO*=100 mm to 25 mm at *SO*=350 mm.

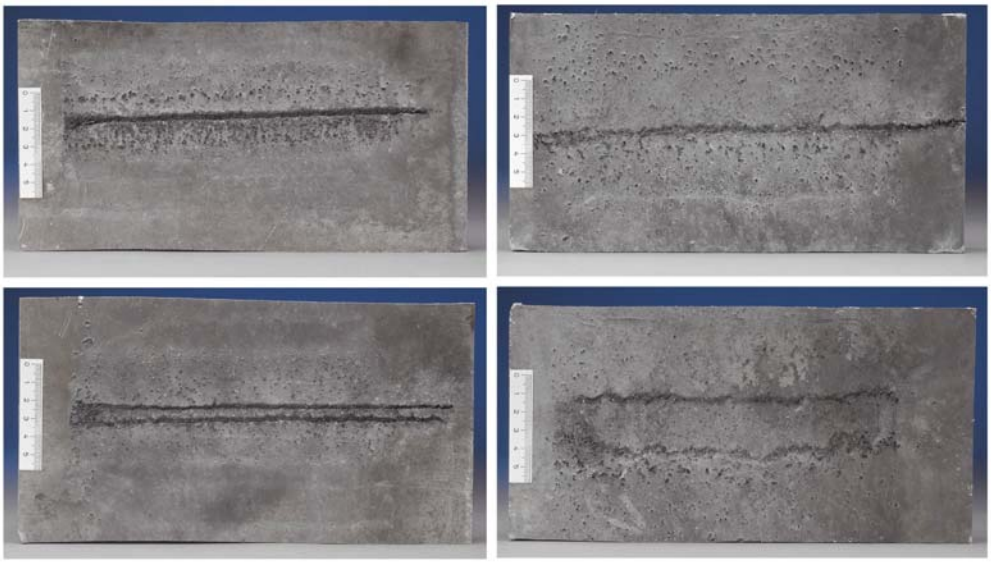

Figure 3. Batch #1 @ 100 mm (above left) and 250 mm (above right)
Batch #2 @ 100 mm (bottom left) and 350 mm (bottom right)

NUMERICAL SIMULATIONS

Numerical simulations using the Euler module of the OTI*HULL software [1] were carried out. This multi-materials hydrocode features a second-order numerical scheme to solve dynamic continuum mechanics problems in finite difference form.

The detonation products are described using a Jones-Wilkins-Lee (JWL) equation of state (see coefficients in Table 1). The detonation velocity is 8030 m/s.

Table 1. Modeling of the explosive

ρ_0 (g/cm^3)	JWL Coefficients					E_0 (GPa cm^3 / cm^3)
	A (GPa)	B (GPa)	R_1	R_2	ω	
1.50	591.20	8.67	4.6	1.2	0.35	8.00

Both the liner and the targets are treated using an elastic-plastic constitutive law based on the Von Mises yield criterion and the Mie-Gruneisen equation of state.

Table 2. Modeling of the inert materials

Material	ρ_0 (g/cm^3)	ν	Y (MPa)	γ_0	$U_s = C_0 + S\,U_p$	
					C_0 (m/s)	S
Lead	11.34	0.30	30	2.00	2092	1.452
Aluminum	2.71	0.33	290	2.10	5380	1.337
HHS	7.86	0.26	1500	1.67	4610	1.730

The first simulation deals with a 3D theoretical geometry, 100 mm in length. There is a symmetry plane so that only half a LSC is modeled. The ignition is at one end. The grid features about 1,700,000 cells. The volume of most interest is meshed using cells of size 0.25x0.25x0.50 mm^3. The mesh is gradually coarsened away from this zone.

Figure 4 shows selected times of the functioning of this reference LSC. The run starts (t=0 µs) with ignition of the explosive at the "rear" end. The detonation emerges at the opposite end at around 12 µs. The first signs of failure appear while the tip of the veil is about 8 mm from the basis of the LSC. The front-views integrate all that happened "behind" the visualization face. From 16 µs they show the detonation products passing through the veil that failed near the ignition end of the LSC.

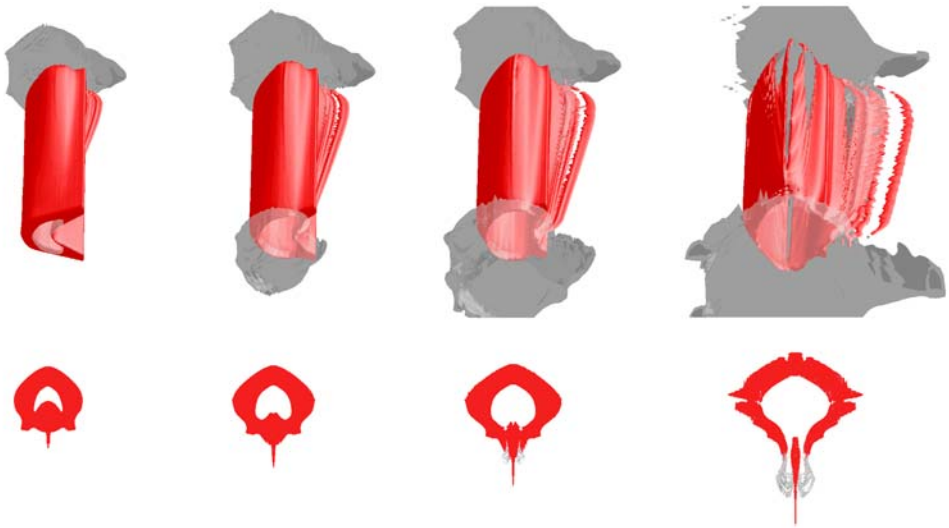

Figure 4. Snapshots of the 3D simulation @ 12, 16, 20 and 30 µs

2D planar numerical simulations were then carried out. They were exploratory calculations on the effects of a calibrated geometrical default upon the functioning of the LSC. A much finer meshing is allowed since only a section of the LSC is modeled. On the other hand the longitudinal component of the velocity of the veil is lost. The entire section of the explosive is simultaneously lightened. The aluminum witness plate, width 120 mm and thickness 30 mm, is located at various stand-off (*SO* = 0 - 30 - 60 mm). The area of most interest is meshed using a subgrid with cells of size 0.05x0.05 mm^2 (400 cells per mm^2). The mesh is then gradually coarsened away from this zone. Depending on the stand-off considered, the mesh size varies from 440,000 cells to more than 740,000 cells. A 3D mesh with the same grid density would involve more than 1,000,000,000 cells.

Particles (immaterial tracers) were inserted in a part of the liner to follow the material flow during the shaping of the veil. This part corresponds to a linear mass of lead of about 65 g/m.

The default consisted in a misalignment of the explosive charge with the liner. The explosive part is moved from 0.1mm "downwards" referring Figure 5 lay-out.

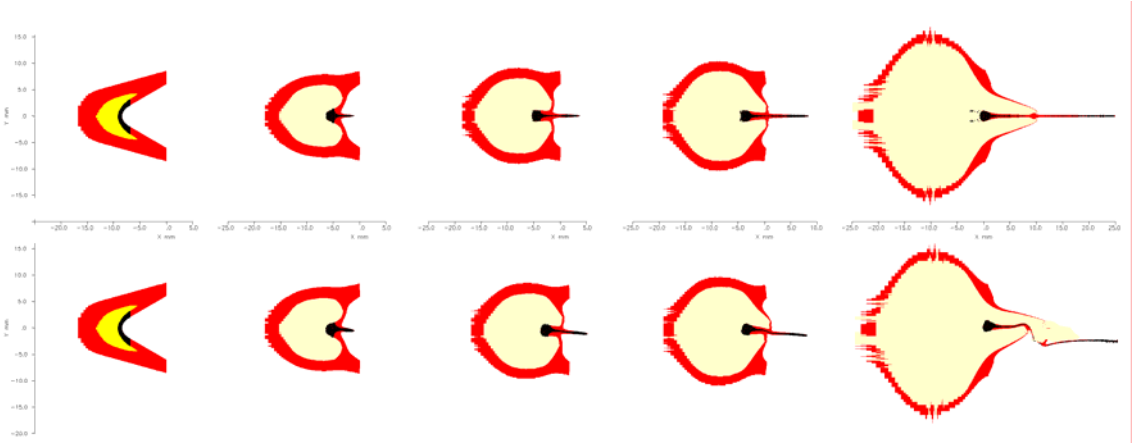

Figure 5. Shaping of the veil with reference LSC (above) and defective LSC (bottom) @ 0-5-7.5-10-20 µs

Figure 5 compares the first 20 microseconds of the veil formation with the reference geometry and the defective geometry. For rigorous comparison, the reference LSC was modelled without any symmetry plane. 5 µs after the ignition of the explosive, one can see that veil is deflected in the direction of the default. At 20 µs, the differences are impressive. The defective LSC forms a main veil with an estimated length of 14 mm, and shifted by 2 to 3 mm "downwards". The rear part generates a second distinct veil, shifted by 1 mm "upwards".

At this stage, we carefully do not claim to have identified the imperfection responsible for the anomalies observed during experiments. But the calculations have shown that a 1/10th-mm misalignment was enough to perturb in a significant way the shaping of the veil.

In terms of performance into a 30-mm thick aluminum block, the differences are also obvious (Figure 6). At zero stand-off, the difference is under 20 %: the reference veil penetrates 17 mm while the defective veil penetrates 14 mm; the bottom of the crater is then shifted by 2.5 mm. Here the stand-off is not enough and the interaction with the target occurs too early compared to the stretching of the veil. At stand-off of 30 and 60 mm, the effects are more significant: the target is perforated by the ideal veil while the defective veil penetrates 14 mm and 13 mm respectively. Those drills are shifted by 3 mm and 5 mm "to the left" respectively. Secondary "drills" are also generated: depth of 2.5 mm and shifted by 4 mm "to the right" at *SO*=30 mm, depth 1 mm and shifted by 8 mm "to the right" at *SO*=60 mm. The width of the main drill decreases with increasing stand-off. At zero stand-off, the drill is 1-mm wide at the bottom and 3.4-mm wide at mid-depth. For *SO*= 30 mm and 60 mm, widths are 0.6 mm and 0.3 mm respectively.

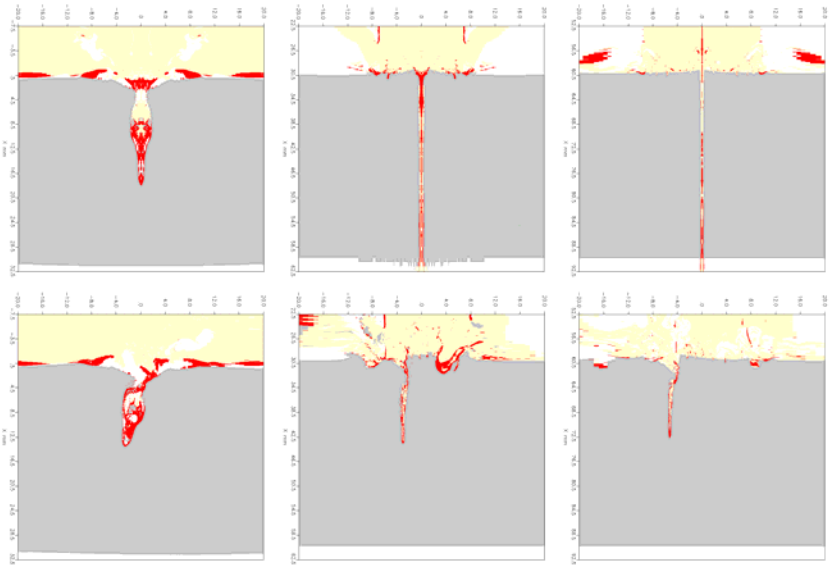

Figure 6. Performance into a 30-mm aluminum plate -
Reference LSC (line above) and defective LSC (line below)
Stand-off of 0 mm (left), 30 mm (middle) and 60 mm (right)

The functional configuration with a steel target at stand-off of 6 mm was finally investigated. The simulation takes into account the light alloy LSC holder. The steel

was modeled as high hardness steel (HHS) with a yield stress of 1500 MPa. The failure behavior of the target was treated using the "P/Y failure curve" capability of the code. It is recognized that strain to failure of ductile high-strength steels depends markedly on the triaxial stress-state which may be characterized by P/Y, where P represents the mean stress or pressure and Y denotes the effective stress Y = $\sqrt{3J_2}$, J2 referred as the second deviatoric stress invariant. Fracture is initiated when the maximum principal strain exceeds the fracture surface $\lambda = f(P/Y)$. This critical strain to failure is used as a simple instantaneous failure criterion and was successfully used by the past [2].

As the target is harder and the stand-off is reduced, the differences of performance in steel are less obvious than previously in aluminum. Figure 7 shows that the two veils perforate the 8-mm plate. However, one will notice that the perforation with the ideal veil is cleaner. Another calculation indicated that a 10-mm plate is not perforated. It is noteworthy that the quantitative results of these numerical simulations perfectly agree with experimental values known by our client.

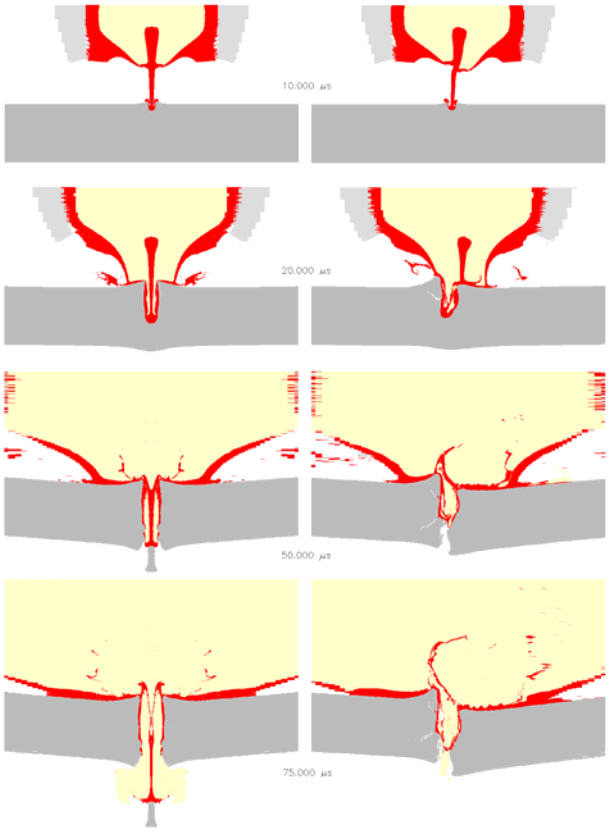

Figure 7. Interaction between the ideal (left) & defective veil (right) with a 8-mm HHS plate (*SO*=6mm)

CONCLUSIONS

A combined experimental and numerical study was carried out to understand why some linear shaped charges had failed qualifying tests for space applications.

Instrumented tests with flash X-Rays revealed veils with an anomaly of curvature. Finally, two parallels drills were successively generated into a witness block of aluminum alloy.

By means of 2D planar Euler numerical simulations with a grid density of 400 cells per square millimeter, the effects of a misalignment of the explosive charge with the liner were examined. The calculations have shown that a $1/10^{th}$-mm misalignment was enough to perturb in a significant way the shaping of the veil. With regard to the stand-off, several drills were then created into a thick block of light alloy. We carefully do not claim to have identified the imperfection responsible for the anomalies observed during experiments.

The effects are less obvious with a thin target made of high hardness steel at a stand-off of 6 mm. Even if the process of interaction differs, the defective linear shaped charge keeps a perforation capacity similar to the ideal reference.

ACKNOWLEDGEMENTS

This work was funded by the French space agency **cnes** *(Centre National d'Etudes Spatiales)* under contract CNES Evry 4700012836/DLA094. The author would like to thank all the technicians who were involved, for their logistical and technical support.

REFERENCES

[1] D.A. Matuska, J.J.Osborn, E.W.Piburn, HULL Users Manual - Version 5, Orlando Technology Inc.
[2] F. Rondot, A predictive numerical tool to determine the limit of perforation of EFPs, *6th International Conference on Mechanical and Physical Behaviour of Materials under Dynamic Loading* EURODYMAT 2000, in *Journal de Physique IV*, **10**, 629-634 (2000)